RESEARCH ARTICLE

Quantum Matter
Vol. 3, 1–4, 2014

Andreev State in Hybrid Superconducting Nanowires

Sergei P. Kruchinin[1,*], Arkadiy Zolotovsky[1], and Hyun Taki Kim[2]

[1]*Bogoliubov Institute for Theoretical Physics, NASU, 14b, Metrologichna Street, Kiev 252143, Ukraine*
[2]*Metal-Insulator Transition Laboratory, Electronics and Telecommunications Research Institute, Daejeon, 305-350, Republic of Korea*

Recent echnology and experiments have fabricated high-quality superconducting hybrid nanowires. We studied hybrid nanowires in wich normal and superconducting regions are in close proximity using the Bogoliubov-de Gennes eqiations for superconductivity in a cylindrical nanowire. We succeeded to obtain the quantum energy levels and wave functions of a superconducting nanowire.

Keywords:

1. INTRODUCTION

Recent advances in nanoscience have demonstrated that fundamentally new physical phenomena are found when systems are reduced in size to dimensions which become comparable to the fundamental microscopic length scales of the investigated material. Superconductivity is a macroscopic quantum phenomenon, and therefore it is especially interesting to see how this quantum state is influenced when the samples are reduced to nanometer sizes. In such systems, new states of matter can be engineered which do not occur in bulk materials. A good example is the case of nanostructures composed of both superconducting and ferromagnetic metals. Here the proximity effects couple the Cooper pair condensate to the spin polarized bandstructure of a ferromagnet, allowing the local coexistence of both pairing and magnetism. In the bulk, the possibility of such a coexistence was examined by Larkin–Ovchinnikov[1] and Fulde–Ferrell,[2] giving the so-called LOFF state. But it has proved difficult to find this state in bulk materials, possibly because it is very sensitive to disorder.[3,4]

In this paper we consider composite nanowires made from both superconducting and ferromagnetic metals. We consider the cylindrical geometry shown in Figure 1, in which one metal forms the core of a nanowire and the second forms the outer cylindrical sheath. Mesoscopic wires with a similar geometry have been examined by Mota and coworkers.[5–8] In those experiments a superconducting Nb or Ta wire of the typical radius $R_1 = 10$–$20\ \mu$m was coated with a thin layer of normal metal (Ag or Cu) of 34–15 μm in thickness. In this work we mainly consider the reverse situation, in which a normal or ferromagnetic core is surrounded by a superconducting sheath. In this case it is interesting to examine the spectrum of Andreev bound states in the normal or ferromagnetic core. The situation is somewhat analogous to a vortex core in a type II superconductor. We can compare the Andreev states in the central cylinder to the well-known Caroli–Matricon[9] quasiparticle states of a vortex core and, hence, consider changes in the spectrum as a function of both the trapped magnetic flux and the physical size of a nanowire. In the case of a ferromagnetic core we can compare the spectrum with results for planar hybrid S/F nanostructures, as reviewed recently by Lyuksyutov and Pokrovsky[10] and by Buzdin.[11] We mention the recent work on the superconductivity of ferromagnetic wires by Wang et al.[12] which presents the significant results on the anomalous effect of proximity revealed in superconducting magnetic wires. We also emphasize the promising direction in the fabrication of MgB_2 nanowires.[13]

2. MODEL

We model the hybrid superconductor-ferromagnet nanowire system by extending the self-consistent theory of a type II vortex developed by Gygi and Schlüter[14] to the case of a ferromagnetic vortex core. We start with the effective Pauli Hamiltonian for the spin-polarized electronic states of a normal metal

$$\hat{H}^0_{\sigma\sigma'} = \frac{(\hat{p} + e\mathbf{A})^2}{2m_e}\delta_{\sigma\sigma'} + V_{\sigma\sigma'}(\mathbf{r}) \tag{1}$$

where $-e$ is the electron charge, $\mathbf{A}(\mathbf{r})$ is the magnetic vector potential, and $V_\sigma(\mathbf{r})$ is a general spin-dependent single potential, where σ is $\uparrow$ / $\downarrow$. This potential could be assumed to be the sum of the ionic, Hartree, and exchange-correlation potentials of

*Author to whom correspondence should be addressed.

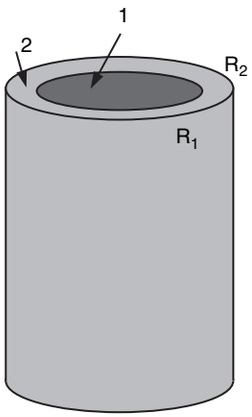

Fig. 1. Nanowire.

a self-consistent spin-polarized DFT calculation, in which case it would have the form

$$V_\sigma(\mathbf{r}) = V_{\text{ion}}(\mathbf{r}) + V_H(\mathbf{r}) + V_{xc}(\mathbf{r}) + \mu_B(\mathbf{B}+\mathbf{B}_{xc})\sigma_{\sigma\sigma'} \quad (2)$$

where $V_{xc}(\mathbf{r})$ is the spin-independent part of the exchange-correlation potential, μ_B is the Bohr magneton, $\mathbf{B}(\mathbf{r})$ is the physical local magnetic field, and $\mathbf{B}_{xc}$ is an effective magnetic field representing the exchange field of the spin-polarization in the ferromagnet. Here $\sigma_{\sigma\sigma'}$ is the vector of Pauli matrices.

To model the superconducting elements of the hybrid system, this single-particle Hamiltonian is supplemented by an effective attraction, which we take as the BCS contact form

$$V(\mathbf{r},\mathbf{r}') = -g(\mathbf{r})\delta(\mathbf{r}-\mathbf{r}') \quad (3)$$

where $g(\mathbf{r})$ is the local attractive potential strength at $\mathbf{r}$. This will be zero in the normal or ferromagnetic part of the nanowire and a constant g in the superconducting parts. For simplicity we neglect a retardation of the attraction in the rest of this paper. The full effective Hamiltonian for our system is

$$\hat{H} = \int d^3r \Big[\sum_{\sigma\sigma'} (\hat{\psi}^+_\sigma(\mathbf{r})\hat{H}^0_{\sigma\sigma'}\hat{\psi}_{\sigma'}(\mathbf{r})) - g(\mathbf{r})\hat{\psi}^+_\uparrow(\mathbf{r})\hat{\psi}^+_\downarrow(\mathbf{r})\hat{\psi}_\downarrow(\mathbf{r})\hat{\psi}_\uparrow(\mathbf{r}) \Big] \quad (4)$$

Here, $\hat{\psi}^+_\sigma(\mathbf{r})$ and $\hat{\psi}_\sigma(\mathbf{r})$ are the usual field operators for the electrons. In the Hartree–Fock–Gorkov approximation, this Hamiltonian is diagonalized by a spin-dependent Bogoliubov–Valatin transformation.

$$\hat{\psi}_\sigma(\mathbf{r}) = \sum_n \left(u_{n\sigma}(\mathbf{r})\hat{\gamma}_n + v^*_{n\sigma}(\mathbf{r})\hat{\gamma}^+_n\right) \quad (5)$$

$$\hat{\psi}^+_\sigma(\mathbf{r}) = \sum_n \left(u^*_{n\sigma}(\mathbf{r})\hat{\gamma}^+_n + v_{n\sigma}(\mathbf{r})\hat{\gamma}_n\right) \quad (6)$$

The requirement that the quasiparticle creation and annihilation operators retain the fermion anticommutation laws,

$$\{\hat{\gamma}_n, \hat{\gamma}^+_{n'}\} = \delta_{nn'} \quad (7)$$

implies that

$$\sum_{n\sigma}(u^*_{n\sigma}(\mathbf{r})u_{n\sigma'}(\mathbf{r}') + v_{n\sigma}(\mathbf{r})v^*_{n\sigma'}(\mathbf{r}')) = \delta(\mathbf{r}-\mathbf{r}')\delta_{\sigma\sigma'} \quad (8)$$

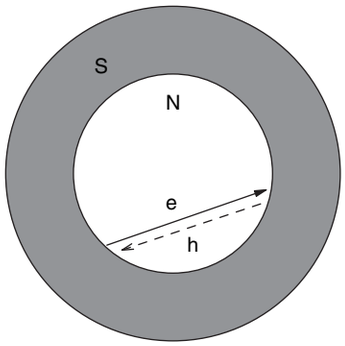

Fig. 2. Billiard 1.

The resulting set of Bogoliubov–de Gennes equations is

$$\begin{pmatrix} \hat{H}_1+V_{\uparrow\uparrow} & V_{\uparrow\downarrow} & 0 & \Delta(\mathbf{r}) \\ V_{\downarrow\uparrow} & \hat{H}_1+V_{\downarrow\downarrow} & -\Delta(\mathbf{r}) & 0 \\ 0 & -\Delta^*(\mathbf{r}) & -\hat{H}_1-V_{\uparrow\uparrow} & -V_{\uparrow\downarrow} \\ \Delta^*(\mathbf{r}) & 0 & -V_{\downarrow\uparrow} & -\hat{H}_1-V_{\downarrow\downarrow} \end{pmatrix} \times \begin{pmatrix} u_{n\uparrow\sigma} \\ u_{n\downarrow\sigma} \\ v_{n\uparrow\sigma} \\ v_{n\downarrow\sigma} \end{pmatrix} = E_{n\sigma} \begin{pmatrix} u_{n\uparrow\sigma} \\ u_{n\downarrow\sigma} \\ v_{n\uparrow\sigma} \\ v_{n\downarrow\sigma} \end{pmatrix} \quad (9)$$

where $\hat{H}_1 = (\hat{p}+e\mathbf{A})^2/2m_e - \mu$ and μ is the chemical potential.

The self-consistent pairing potential corresponds to a pure spin-singlet pairing state and is given by

$$\Delta(\mathbf{r}) = g\langle\hat{\psi}_\uparrow(\mathbf{r})\hat{\psi}_\downarrow(\mathbf{r})\rangle \quad (10)$$

In the special case where the magnetization of the ferromagnet is in the same collinear direction, $\mathbf{B}_{xc}$, as the external field $\mathbf{B}$, choosing it as the spin-quantization axis $\hat{z}$, we have $V_{\uparrow\downarrow} = V_{\downarrow\downarrow} = 0$. In this case the full set of four matrix Bogliubov–de Gennes equations separates into a pair of 2×2 matrix equations

$$\begin{pmatrix} \hat{H}_1+V_{\uparrow\uparrow} & \Delta(\mathbf{r}) \\ \Delta^*(\mathbf{r}) & -\hat{H}_1-V_{\downarrow\downarrow} \end{pmatrix} \begin{pmatrix} u_{n\uparrow\sigma} \\ v_{n\downarrow\sigma} \end{pmatrix} = E_{n\sigma} \begin{pmatrix} u_{n\uparrow\sigma} \\ v_{n\downarrow\sigma} \end{pmatrix} \quad (11)$$

$$\begin{pmatrix} \hat{H}_1+V_{\downarrow\downarrow} & -\Delta(\mathbf{r}) \\ -\Delta^*(\mathbf{r}) & -\hat{H}_1-V_{\uparrow\uparrow} \end{pmatrix} \begin{pmatrix} u_{n\downarrow\sigma} \\ v_{n\uparrow\sigma} \end{pmatrix} = E_{n\sigma} \begin{pmatrix} u_{n\downarrow\sigma} \\ v_{n\uparrow\sigma} \end{pmatrix} \quad (12)$$

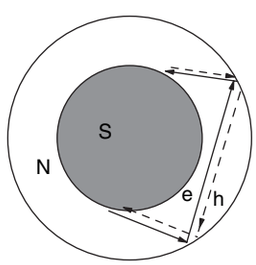

Fig. 3. Billiard 2.

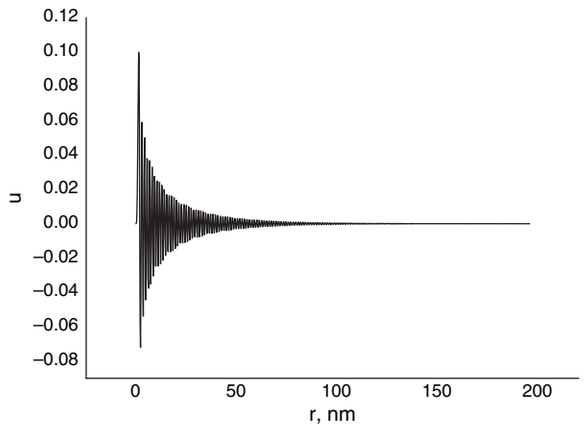

Fig. 4. Quasiparticle amplitude of the andreev state.

3. NUMERICAL CALCULATION

We will study the Bogoliubov–de Gennes equations, by using a numerical method to solve these equations. The calculation algorithm is realized with the use of the most powerful FORTRAN language specially developed for mathematical calculations.

In view of the cylindrical symmetry of the system under study, we write the system of Bogoliubov–de Gennes equations in the form suitable for calculations. We will also use the fact that the amplitudes of the functions $u(r)$ and $v(r)$ tend to zero at the boundary point. The solutions of the equations are determined with the use of the Runge–Kutta method.

Taking the symmetry of our system (cylindrical) to account and choosing the gauge in which the parameter $\Delta(r)$ is real, we can write the system of Bogoliubov–de Gennes equations in the form

$$\begin{aligned}\bar{u}(r,\theta,z) &= u_{\mu nk_z}(r)e^{-i\mu\theta}e^{-ik_z z}\\ \bar{v}(r,\theta,z) &= v_{\mu nk_z}(r)e^{i\mu\theta}e^{-ik_z z}\end{aligned} \tag{13}$$

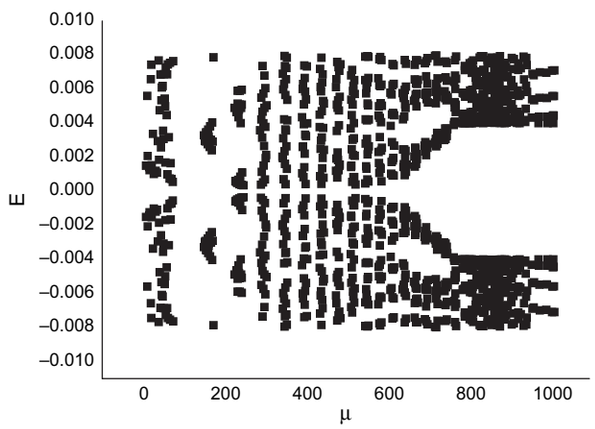

Fig. 5. Andreev spectrum as a function of the angular momentum for billiard 1.

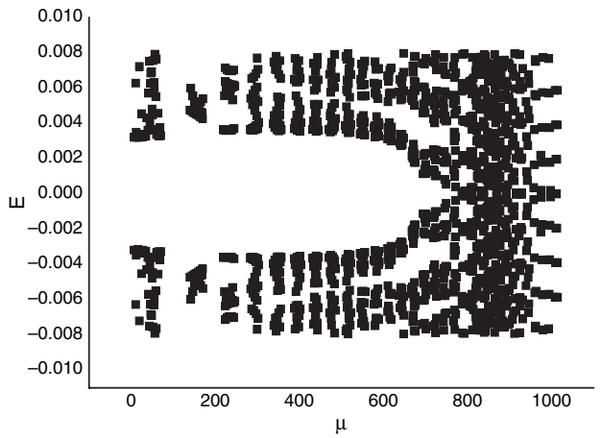

Fig. 6. Andreev spectrum as a function of the angular momentum for billiard 2.

$$\begin{aligned}&-\frac{\partial^2}{\partial r^2}u_{\mu nk_z}(r)-\frac{1}{r}\frac{\partial}{\partial r}u_{\mu nk_z}(r)\\&\quad+U(r)\cdot u_{\mu nk_z}(r)+\Delta(r)\cdot v_{\mu nk_z}(r)=0\\&-\frac{\partial^2}{\partial r^2}v_{\mu nk_z}(r)-\frac{1}{r}\frac{\partial}{\partial r}v_{\mu nk_z}(r)\\&\quad+U(r)\cdot v_{\mu nk_z}(r)-\Delta(r)\cdot u_{\mu nk_z}(r)=0\end{aligned} \tag{14}$$

where $U(r)=\mu^2/r^2-(E_f-k_z^2/m_z-E_{\mu nk_z})$.

The plot of wave functions is given in Figure 4 ($E_0 = 3.198136337995529\times10^{-3}$ eV, $E_f = 1$ eV, $\Delta = 0.1$ eV, $k_z = 0$, $R_1 = 150$ nm, $R_2 = 200$ nm, $\mu = 1$). In Figures 5 and 6, we present the results of calculations for the spectrum of Andreev states of the system.

The resulting spectrum as a function of the angular momentum is shown in Figure 5 for billiard 1 (Fig. 2). The resulting spectrum as a function of the angular momentum is shown in Figure 6 for billiard 2 (Fig. 3). The spectrum demonstrates the splitting caused by the boundary effect.

4. DISCUSSION

The Andreev-billiard systems are the analog of a classical billiard. The Andreev billiard is interpreted as a ballistic motion

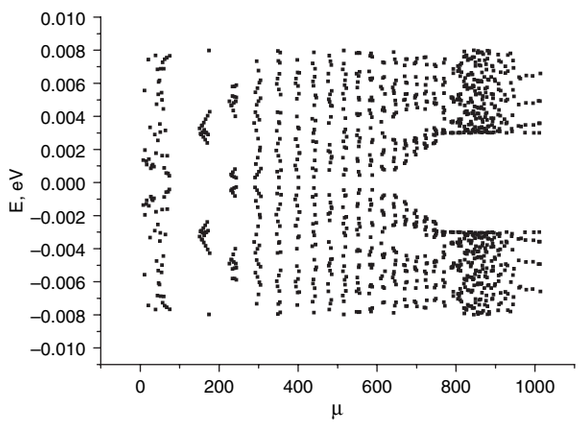

Fig. 7. Andreev spectrum for MgB_2 nanowires (billiard 1).

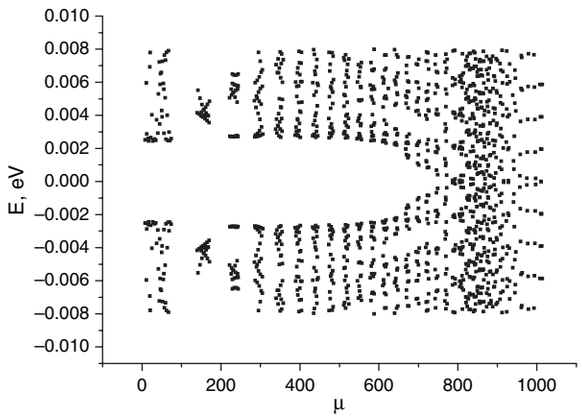

Fig. 8. Andreev spectrum for MgB_2 nanowires (billiard 2).

with the Andreev reflection at the interface with a superconductor. The Andreev reflection is a fundamental process that converts an electron incident on a superconductor into a hole while a Cooper pair is added to the superconductivity condensate. Figures 5 and 6 demonstrate the electron–hole symmetry of the Andreev spectrum. One-dimensional solutions of the Bogoliubov–de Gennes equations pass into in two-dimensional ones with increase in μ. It is worth noting that we work in the clean limit (mean free path $l \gg \lambda, \xi$).

Estimates of the penetration depth and the length scale of order were performed in Ref. [15]:

$$\begin{cases} \lambda(T) = \dfrac{\lambda_0}{\sqrt{1-t^4}} \quad \text{where } t = \dfrac{T}{T_c} \\ \xi(T) = \dfrac{\xi_0(1-0.25t)}{\sqrt{1-t}} \end{cases} \tag{15}$$

where $\lambda_0 = 46$ nm and $\xi_0 = 74$ nm, i.e., almost the characteristic lengths of lead at zero temperature in the clean limit. We have carried out also the calculations for MgB_2 nanowires with the parameters ($R_1 = 150$ nm, $R_2 = 200$ nm, $k_z = 0$, $\Delta = 0.003$ eV, $E_f = 1$ eV). In Figure 7 ($R_1 = 150$ nm, $R_2 = 200$ nm, $k_z = 0$, $\Delta = 0.003$ eV, $E_f = 1$ eV), we present the spectrum as a function of the angular momentum for MgB_2 nanowires (billiard 1), whereas Figure 8 shows the analogous dependence in the case of billiard 2.

5. CONCLUSIONS

We studied hybrid nanowires in which normal and superconducting regions are in close proximity, by using the Bogoliubov–de Gennes equations for superconductivity in a cylindrical nanowire. We developed a method for numerical solutions of these equations in FORTRAN programme and obtained some preliminary results. We succeeded to obtain the quantum energy levels and wave functions of a superconducting nanowire. The spectrum of states we calculated shows the interesting "Andreev Billiard" characteristics. Preliminary results were also obtained for the cases of a magnetic nanowire and a superconducting nanowire containing a vortex. The calculations for a superconducting nanowire can be extended to the cases of a superconductor-ferromagnet hybrid nanowire and a nanowire containining one or more superconducting flux quanta.[12,17–20]

Within this approach, the problems of BEC and nanowires can be considered as well.[16]

Acknowledgment: We thank for support the Ukraine–Korea project no. 376.

References and Notes

1. A. Larkin and Y. Ovchinnikov, *Sov. Phys. JETP* 20, 762 **(1965)**.
2. P. Fulde and A. Ferrell, *Phys. Rev.* 135, A550 **(1964)**.
3. S. Kruchinin, H. Nagao, and S. Aono, Modern Aspects of Superconductivity: Theory of superconductivity, World Scientific, Singapore **(2010)**, p. 220.
4. S. Kruchinin and H. Nagao, *Inter. J. Mod. Phys. B* 26, 1230013 **(2012)**.
5. A. C. Mota, P. Visani, A. Polloni, and K. Aupke, *Physica B* 197, 95 **(1994)**.
6. F. B. Müller-Allinger, A. C. Mota, and W. Belzig, *Phys. Rev. B* 59, 8887 **(1999)**.
7. F. B. Müller-Allinger and A. C. Mota, *Phys. Rev. Lett* 84, 3161 **(2000)**.
8. F. B. Müller-Allinger and A. C. Mota, *Physica B* 284–288, 683 **(2000)**.
9. C. Caroli and J. Matricon, *Phys. Kondens. Mater.* 3, 380 **(1965)**.
10. I. F. Lyuksyutov and V. L. Pokrovsky, *Adv. Phys.* 54, 67 **(2005)**.
11. A. I. Buzdin, *Rev. Mod. Phys.* 77, 935 **(2005)**.
12. J. Wang, et al., *Nature Phys.* 6, 389 **(2010)**.
13. Portesi, et al., *J. Phys: Condens. Matter.* 20, 8 **(2008)**.
14. F. Gygi and M. Schluter, *Phys. Rev. B* 43, 7609 **(1991)**.
15. G. Stenuit, et al., *Eur. Phys. J. B.* 33, 103 **(2003)**.
16. A. A. Shanenko, D. Croitoru, A. Vagov, and M. Peeters, *Proceedings of NATO ARW Physical Properties of nanosystems*, edited by J. Bonca and S. Kruchinin, Springer **(2008)**, pp. 340–348.
17. P. K. Bose, N. Paitya, S. Bhattacharya, D. De, S. Saha, K. M. Chatterjee, S. Pahari, and K. P. Ghatak, *Quantum Matter* 1, 89 **(2012)**.
18. B. Tüzün and C. Erkoç, *Quantum Matter* 1, 136 **(2012)**.
19. T. Ono, Y. Fujimoto, and S. Tsukamoto, *Quantum Matter* 1, 4 **(2012)**.
20. M. Narayanan and A. J. Peter, *Quantum Matter* 1, 53 **(2012)**; Paitya, S. Bhattacharya, and K. P. Ghatak, *Quantum Matter* 1, 63 **(2012)**.

Received: 3 February 2013. Accepted: 19 February 2013.